nature nanotechnology

LETTERS

PUBLISHED ONLINE: 14 MARCH 2016 | DOI: 10.1038/NNANO.2016.23

Aggregated single-walled carbon nanotubes attenuate the behavioural and neurochemical effects of methamphetamine in mice

Xue Xue[1†], Jing-Yu Yang[2†], Yi He[3†], Li-Rong Wang[1,4], Ping Liu[2], Li-Sha Yu[2], Guo-Hua Bi[3], Ming-Ming Zhu[2], Yue-Yang Liu[2], Rong-Wu Xiang[5], Xiao-Ting Yang[2], Xin-Yu Fan[2], Xiao-Min Wang[2], Jia Qi[3], Hong-Jie Zhang[6], Tuo Wei[1,7], Wei Cui[2], Guang-Lu Ge[1,4], Zheng-Xiong Xi[3]*, Chun-Fu Wu[2]* and Xing-Jie Liang[1,7]*

Methamphetamine (METH) abuse is a serious social and health problem worldwide. At present, there are no effective medications to treat METH addiction[1]. Here, we report that aggregated single-walled carbon nanotubes (aSWNTs) significantly inhibited METH self-administration, METH-induced conditioned place preference and METH- or cue-induced relapse to drug-seeking behaviour in mice. The use of aSWNTs alone did not significantly alter the mesolimbic dopamine system, whereas pretreatment with aSWNTs attenuated METH-induced increases in extracellular dopamine in the ventral striatum. Electrochemical assays suggest that aSWNTs facilitated dopamine oxidation. In addition, aSWNTs attenuated METH-induced increases in tyrosine hydroxylase or synaptic protein expression. These findings suggest that aSWNTs may have therapeutic effects for treatment of METH addiction by oxidation of METH-enhanced extracellular dopamine in the striatum.

Single-walled carbon nanotubes have recently attracted more attention in biomedical research. Owing to their unique electrical, optical and mechanical properties, SWNTs have been widely used in nanoelectronics, biosensors and nanocarriers for cancer therapies[2,3]. In contrast to their wide implications, little is known about the biological effects of the SWNTs themselves. We and others have reported that low doses of SWNTs are neuroprotective in animal models of Alzheimer's disease[4] and strokes[5]; SWNTs were also reported to alter mitochondrial function and intracellular energy metabolism[6,7]. Strikingly, recent studies showed that nanoparticle-coated electrodes are highly sensitive and effective in the adsorption and oxidation of dopamine, largely through increasing the electroactive surface areas[8–10]. Given the important roles of dopamine in the regulation of locomotion and goal-directed motivational behaviours such as drug abuse and addiction[11], we hypothesized that SWNTs might be useful for the treatment of drug addiction by rapidly adsorbing and oxidizing the extracellular dopamine produced by drugs of abuse. METH is a highly potent psychostimulant and a dopamine releaser[12]. We therefore investigated the effects of SWNTs on METH-enhanced extracellular dopamine and METH addiction-related behaviour.

There are two types of SWNTs—individual SWNTs (iSWNTs) and aggregated SWNTS (aSWNTs)—which exhibit different bioactivities, as we demonstrated previously[7]. iSWNTs have an average size of 1–2 nm × 0.1–1 μm, whereas aSWNTs form aggregated bundles with average sizes of 15–20 nm × 0.1–1 μm (Supplementary Fig. 1a,b). The length distribution, ratio of metallic and semiconducting SWNTs and the low disordered carbon signal to graphitic signal bands (D/G ratio) of both types of SWNTs (Supplementary Fig. 1c,d) are similar to values in the literature[7].

As it is difficult to penetrate the blood–brain barrier, SWNTs were injected locally into a lateral cerebral ventricle in this study. We first evaluated the potential neural toxicity of intracerebroventricular (i.c.v.) microinjection of SWNTs in mice. Supplementary Fig. 2 shows that i.c.v. microinjection of iSWNTs or aSWNTs (1 or 2 ng) had no effect on animal body weight, feeding, drinking or locomotor behaviour compared with the vehicle (0.01% sodium deoxycholate in artificial cerebrospinal fluid) control group. There was no detectable alteration in cellular morphology in the prefrontal cortex (PFC) or striatum as assessed by hematoxylin and eosin staining of cell nuclei or terminal deoxynucleotidyl transferase dUTP nick end labelling (TUNEL)-staining of DNA fragments 24 h or 2 weeks after SWNT administration (Supplementary Fig. 3). We then examined the effects of SWNTs on the mesolimbic dopamine system. We did not find significant changes in either tyrosine hydroxylase (TH)- or dopamine transporter (DAT)-immunostaining in the midbrain of mice after SWNT administration (Supplementary Fig. 4a–c). SWNTs also failed to alter striatal dopamine contents (Supplementary Fig. 4d) or the expression of TH, DAT or vesicular monoamine transporter 2 (VMAT2) in the striatum (Supplementary Fig. 4e). These findings suggest that i.c.v. microinjection of SWNTs alone had no significant adverse effects on general behaviour or on the mesolimbic dopamine system.

It is well documented that the rewarding and psychostimulating effects of METH are mediated by the activation of the mesolimbic dopamine system, in which METH causes a massive dopamine release in the projection areas of the brain such as the ventral striatum and PFC[12]. Given the unique tubular structure of SWNTs with rich carboxyl groups exposed and extremely large surface areas[9,10], we hypothesized

[1]CAS Center for Excellence in Nanoscience, Chinese Academy of Sciences and National Center for Nanoscience and Technology of China, Beijing 100190, China. [2]Department of Pharmacology, Shenyang Pharmaceutical University, Shenyang 110016, China. [3]Intramural Research Program, National Institute on Drug Abuse, National Institutes of Health, Baltimore, Maryland 21224, USA. [4]CAS Key Laboratory of Standardization and Measurement for Nanotechnology, National Center for Nanoscience and Technology of China, Beijing 100190, China. [5]Department of Biopharmaceutical Information, Shenyang Pharmaceutical University, Shenyang 110016, China. [6]State Key Laboratory of Biomacromolecules, Institute of Biophysics, Chinese Academy of Sciences, Beijing 100101, China. [7]CAS Key Laboratory for Biomedical Effects of Nanomaterials and Nanosafety, National Center for Nanoscience and Technology of China, Beijing 100190, China. †These authors contributed equally to this work. *e-mail: zxi@mail.nih.gov; wucf@syphu.edu.cn; liangxj@nanoctr.cn

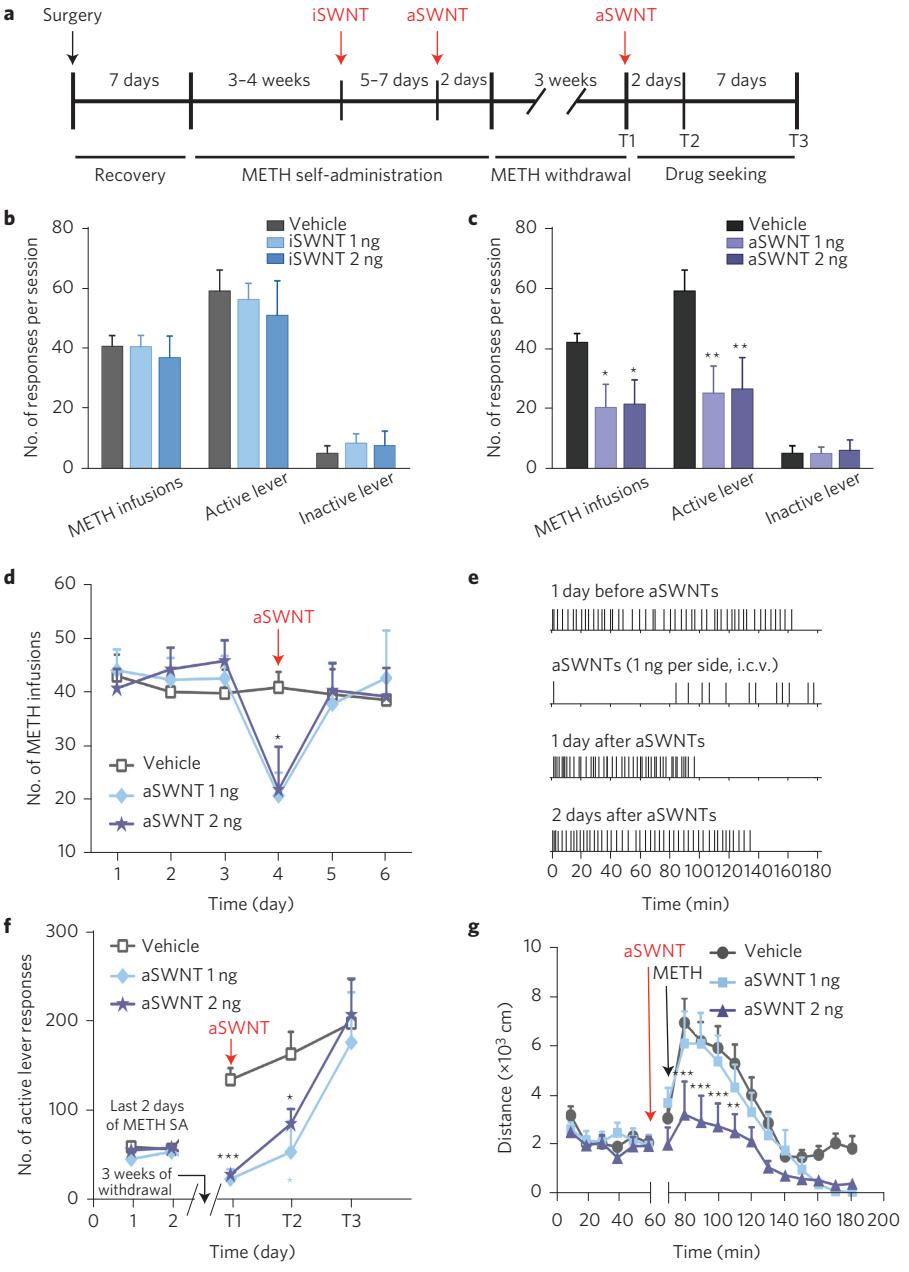

Figure 1 | Effects of SWNTs on METH self-administration, cue-induced METH-seeking and METH-enhanced locomotion in mice. a, Timeline of the METH self-administration and relapse experiments. **b**, Microinjection of iSWNTs (1 or 2 ng 30 min before testing) had no effect on METH self-administration compared with the vehicle (0.01% sodium deoxycholate in artificial cerebrospinal fluid) control group (METH infusions: $F_{2,25} = 0.22$, $p > 0.05$; active lever presses: $F_{2,25} = 0.41$, $p > 0.05$, one-way ANOVA; the values of F refer to the degrees of freedom in group number and independent observations). **c**, Microinjection of aSWNTs significantly inhibited METH self-administration (METH infusions: $F_{2,25} = 3.92$, $p < 0.05$; active lever presses: $F_{2,25} = 4.40$, $p < 0.05$). **d**, Time courses of the action produced by aSWNTs. **e**, Representative METH self-administration records, indicating that aSWNTs caused cessation of METH self-administration on the test day. Each vertical line represents one METH infusion. **f**, aSWNT pretreatment inhibited cue-induced drug seeking in mice after 3 weeks of withdrawal from previous METH self-administration. Two-way ANOVA with repeated measures over time revealed a significant aSWNT treatment main effect ($F_{2,25} = 12.95$, $p < 0.001$, statistically significant difference across all treatment groups) and time main effect ($F_{2,46} = 27.00$, $p < 0.001$, statistically significant difference across all the time points). **g**, Pretreatment with aSWNTs also inhibited 1 mg kg^{-1} METH-induced increase in locomotion ($F_{2,23} = 6.88$, $p < 0.01$). The error bars indicate the standard error of the mean (s.e.m.) from the means of 8–10 mice in each group (see Methods for details). $^{*}p < 0.05$, $^{**}p < 0.01$ and $^{***}p < 0.001$, compared with the vehicle group.

that SWNTs might be effective in the attenuation of METH addiction-related behaviour by rapid adsorption and oxidization of the excess extracellular dopamine due to METH. To test this hypothesis, we first observed the effects of SWNTs on intravenous METH self-administration, one of the most commonly used animal models for studying drug reward and addiction[13]. Figure 1a shows the general experimental procedure. Figure 1b shows that i.c.v. microinjections of iSWNTs into the lateral ventricle (1 or 2 ng, 30 min before the test) had no effect on METH self-administration. However, i.c.v. microinjections of the same doses of aSWNTs produced a significant reduction in METH self-administration (Fig. 1c). This effect lasted less than 24 h (Fig. 1d). Figure 1e shows the patterns of METH self-administration before and after aSWNT administration: the aSWNTs caused cessation of METH self-administration during a 3-hour-long test session.

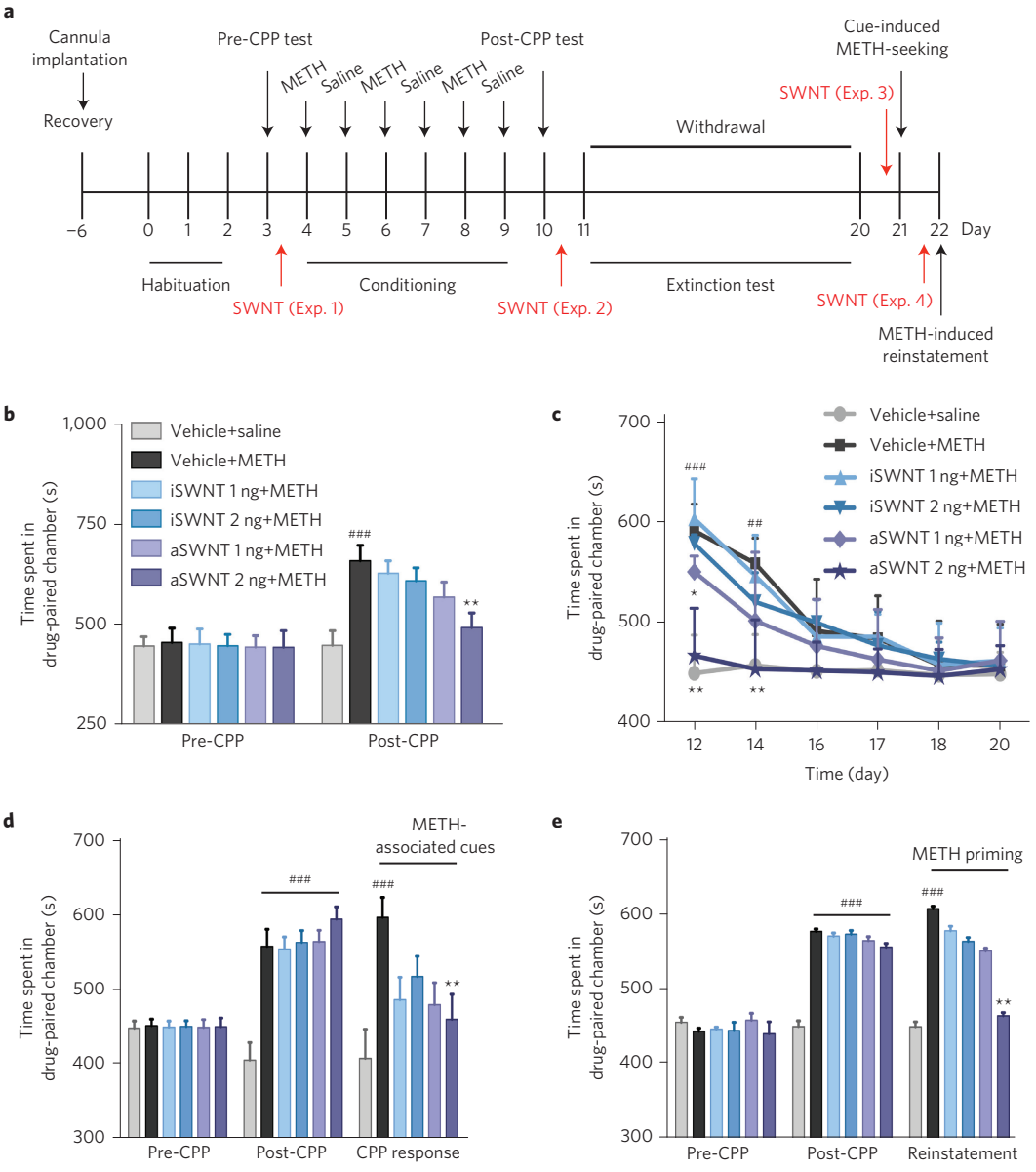

Figure 2 | Effects of SWNTs on METH-induced CPP, extinction of CPP and reinstatement of CPP. a, Timeline for the CPP experiments. Four groups of mice were used to assess the effects of SWNTs on METH-induced CPP (Exp. 1), CPP extinction (Exp. 2), cue-induced CPP response (Exp. 3), and METH-induced reinstatement of CPP (Exp. 4), respectively. Each group of mice was then randomly divided into 6 subgroups ($n = 7$ mice per subgroup). **b**,**c**, Pretreatment with aSWNTs, but not iSWNTs, inhibited the acquisition of METH-induced CPP (**b**, $F_{5,36} = 5.34$, $p < 0.001$) and facilitated the extinction of METH-induced CPP (**c**, $F_{5,36} = 7.92$, $p < 0.001$). **d**,**e**, Pretreatment with aSWNTs, but not iSWNTs, significantly inhibited the cue-induced CPP response (**d**, $F_{5,36} = 4.48$, $p < 0.001$) and METH-induced reinstatement of CPP (**e**, $F_{5,36} = 5.72$, $p < 0.001$). The error bars indicate s.e.m. of the mean from 7 mice in each subgroup. $^{\#\#}p < 0.01$ and $^{\#\#\#}p < 0.001$, compared with the vehicle+saline group (grey bars). $^{*}p < 0.05$, $^{**}p < 0.01$ compared with the vehicle+METH group (black bars).

We then examined the effects of aSWNTs on relapse to drug-seeking behaviour, a key issue in human drug addiction[13,14]. We used the animal model of incubation of craving[14], in which animals were first allowed intravenous METH self-administration and then subjected to three weeks of withdrawal in their home cages. When the animals were re-exposed to the same self-administration chambers, the drug-associated contextual stimuli (cues) induced robust lever-pressing (drug-seeking behaviour) in the absence of METH reinforcement. Pretreatment with aSWNTs (1 or 2 ng by i.c.v. microinjection 30 min before testing) almost completely blocked cue-induced drug-seeking behaviour (Fig. 1f). Such cue-induced drug-seeking was repeated twice on day 3 (T2) and day 10 (T3) after the first test (T1), illustrating that this inhibitory effect lasted at least 3 days and then diminished 10 days after the first relapse test (Fig. 1f). We also examined the effects of aSWNTs on METH-enhanced locomotion. Figure 1g shows that i.c.v. microinjection of aSWNTs inhibited METH-induced increases in locomotion in a dose-dependent manner.

Conditioned place preference (CPP) is another commonly used animal model to assess the rewarding properties of drugs or reward-related memory[13]. The CPP reinstatement test measures the ability of drug-related stimuli to trigger affective craving and relapse to drug-seeking behaviour[13]. Therefore, we used the CPP and reinstatement models (Fig. 2a) to confirm the findings observed in the above self-administration experiments. Before METH injection, animals showed no preference for any particular environment as assessed by

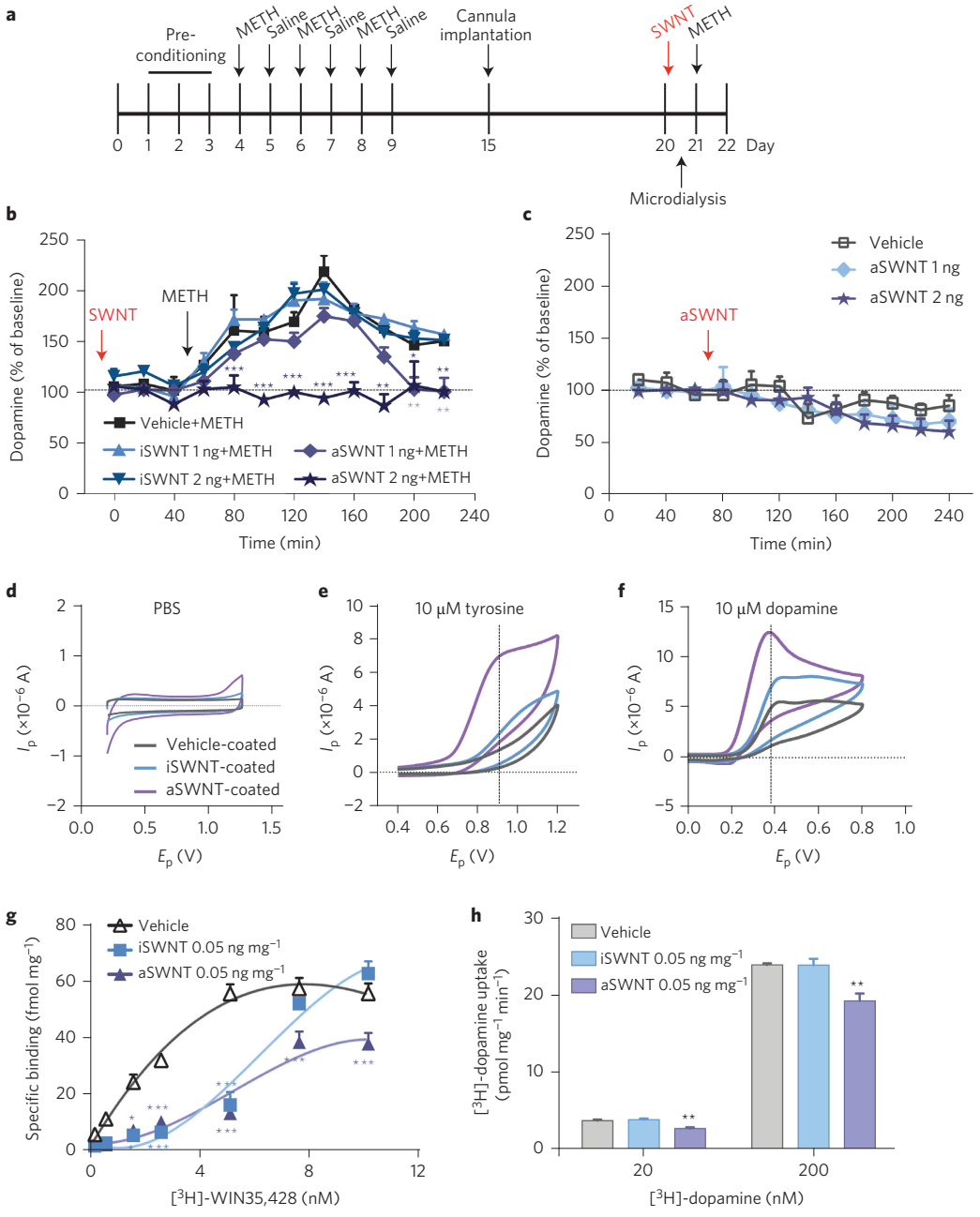

Figure 3 | Effects of SWNTs and METH on extracellular dopamine, dopamine oxidation and dopamine transporter (DAT) binding and function. **a**, Timeline for the microdialysis experiment. **b**, Pretreatment with aSWNTs (1 or 2 ng by i.c.v. microinjection, $n = 12$ mice per group) dose-dependently attenuated METH-enhanced extracellular dopamine in the striatum. Two-way ANOVA with repeated measurements over time revealed a statistically significant SWNT treatment main effect ($F_{4,55} = 43.5$, $p < 0.001$) and time main effect ($F_{11,605} = 76.6$, $p < 0.001$). **c**, aSWNTs (1 or 2 ng by i.c.v. microinjection, $n = 8$ mice per group) alone did not significantly alter the basal levels of extracellular dopamine in the ventral striatum compared with the vehicle control group ($n = 7$ mice per group) ($F_{2,20} = 0.45$, $p > 0.05$). **d**–**f**, Representative fast-cyclic voltammograms, illustrating that SWNT-coated electrodes detected much larger tyrosine (10 μM) or dopamine (10 μM) oxidation currents than uncoated electrodes. I_p, oxidation current; E_p, applied voltage. **g**, Incubation of striatal tissue with aSWNTs (50 μg mg^{-1} tissue) inhibited [^{3}H]-WIN35,428 binding to DAT in the striatal membrane preparations, and shifted the [^{3}H]-WIN35,428 binding curves to the right (the maximal number of DAT binding sites $B_{max} = 78.23 \pm 7.90$ pmol mg^{-1}; the equilibrium dissociation constant $k_d = 3.02 \pm 0.81$ nM). **h**, Incubation with aSWNTs (50 μg mg^{-1} tissue) also reduced re-uptake of [^{3}H]-dopamine in striatal synaptosomes (20 nM: $F_{2,9} = 19.09$, $p < 0.001$; 200 nM: $F_{2,9} = 13.83$, $p < 0.01$, $n = 4$ mice per group). The maximal velocity of dopamine uptake $V_{max} = 6.50 \pm 0.43$ fmol mg^{-1} min^{-1}; the dopamine concentration at 1/2 V_{max} $k_m = 336.3 \pm 68.4$ nM^{-1}. The error bars indicate the s.e.m. of the means from 7–12 animals in each group (**b**,**c**) or from 4 different striatal samples (**g**,**h**). Each striatal sample was replicated three times. *$p < 0.05$, **$p < 0.01$ and ***$p < 0.001$, compared with the vehicle group.

a 15-min pre-CPP test, in which animals spent roughly equivalent amounts of time in both sides of the CPP device (Fig. 2b, left panel). After three paired METH conditioning sessions in a distinctive chamber, the METH-treated group displayed a significant preference to the METH-paired chamber (Fig. 2b, right panel). Pretreatment with aSWNTs (but not iSWNTs) dose-dependently attenuated the acquisition of METH-induced CPP (Fig. 2b, right panel) in one group of mice (Fig. 2a, Exp. 1) and facilitated the extinction of METH-induced CPP in another group of mice (Fig. 2a, Exp. 2; Fig. 2c). In addition, aSWNT pretreatment also inhibited the

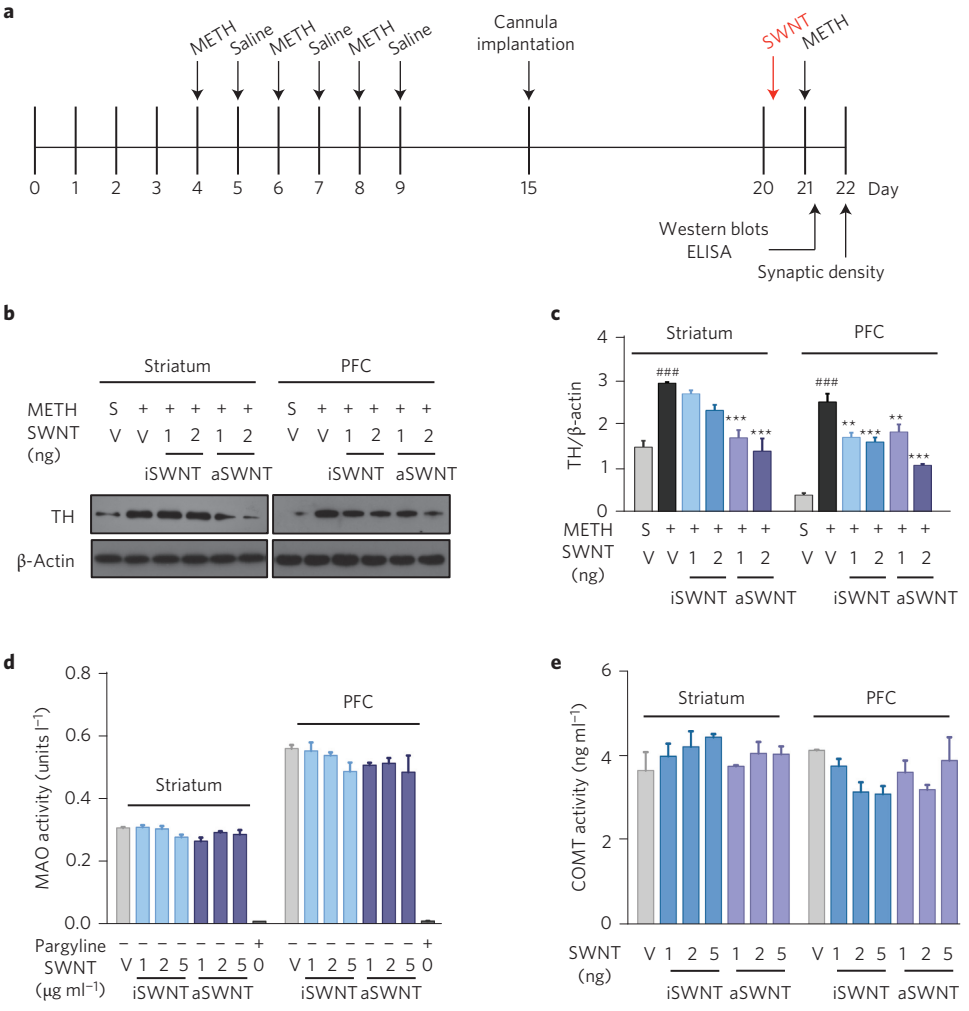

Figure 4 | Effects of SWNTs and METH on the expression of tyrosine hydroxylase (TH) and the activities of dopamine degradation enzymes (MAO and COMT). a, Timeline for the biochemical experiments. **b**,**c**, Representative (**b**) and quantitative (**c**) Western blot assay results, in which the lanes represent the TH or β-actin level in each brain tissue sample as shown above, illustrating that aSWNTs (and iSWNTs to a less extent) significantly attenuated METH-induced increases in TH expression in both the striatum (**c**, $F_{5,12} = 16.59$, $p < 0.001$) and the PFC (**c**, $F_{5,12} = 34.61$, $p < 0.001$). **d**,**e**, ELISA enzyme activity assays, illustrating that SWNT pretreatment did not alter MAO or COMT activities in either the striatum or the PFC when pre-treated with METH in mice. The error bars indicate the s.e.m. of the mean values from 4 brain samples (from 4 mice) in each group. Each brain sample was replicated three times. $^{###}p < 0.001$, compared with the vehicle+saline group (grey bar). $^{**}p < 0.01$, $^{***}p < 0.001$, compared with the vehicle+METH group (black bar). S, saline; V, vehicle.

METH-associated cue-induced CPP response in mice after 10 days of withdrawal from the last METH conditioning (Fig. 2d), and the METH priming-induced reinstatement of CPP in mice after CPP extinction (Fig. 2e). Taken together, these findings from multiple animal models suggest that aSWNTs have significant therapeutic effects in the attenuation of METH reward and relapse to METH-seeking behaviour.

METH-induced dopamine release is mediated by blocking the intracellular VMAT2 that prevents dopamine re-uptake into intracellular vesicles, and therefore facilitates cytoplasmic dopamine release into the extracellular space via DAT[12]. To determine whether dopamine-related mechanisms underlie the above behavioural effects of aSWNTs, we measured the METH-induced changes in extracellular dopamine in the ventral striatum in the presence or absence of SWNTs in mice treated with METH (Fig. 3a). We found that pretreatment with i.c.v. microinjection of aSWNTs, but not iSWNTs, significantly attenuated the METH-induced increase in extracellular dopamine in a dose-dependent manner (Fig. 3b), whereas aSWNTs alone did not significantly alter the extracellular dopamine in the ventral striatum compared with the vehicle control group (Fig. 3c). These findings suggest that a dopamine-dependent mechanism may underlie the behavioural effects of aSWNTs described above.

We then investigated how aSWNTs attenuate METH-enhanced extracellular dopamine. As glassy carbon electrodes coated with nickel oxide nanoparticles or carbon nanotubes are reported to be more sensitive than uncoated electrodes in adsorption and oxidation of dopamine[8–10], we examined the effects of the SWNTs on dopamine oxidization using the same *in vitro* electrochemical methods. Figure 3d–f shows that SWNT-coated electrodes detected much larger tyrosine (a dopamine precursor) or dopamine oxidation currents than vehicle-coated electrodes in the presence of the same concentration (10 μM) of tyrosine or dopamine, suggesting that SWNTs potentiated dopamine oxidation on SWNT-coated electrodes. Notably, aSWNTs were more potent than iSWNTs in this action, which may in part explain the different efficacy of iSWNTs and aSWNTs in the behavioural and neurochemical tests described above.

We also examined the possible interaction between SWNTs and DAT in striatal membrane preparations. Co-administration of SWNTs and [^{3}H]-WIN35,428, a selective DAT inhibitor, significantly decreased [^{3}H]-WIN35,428 binding to striatal DAT and shifted the dose–response binding curve to the right and

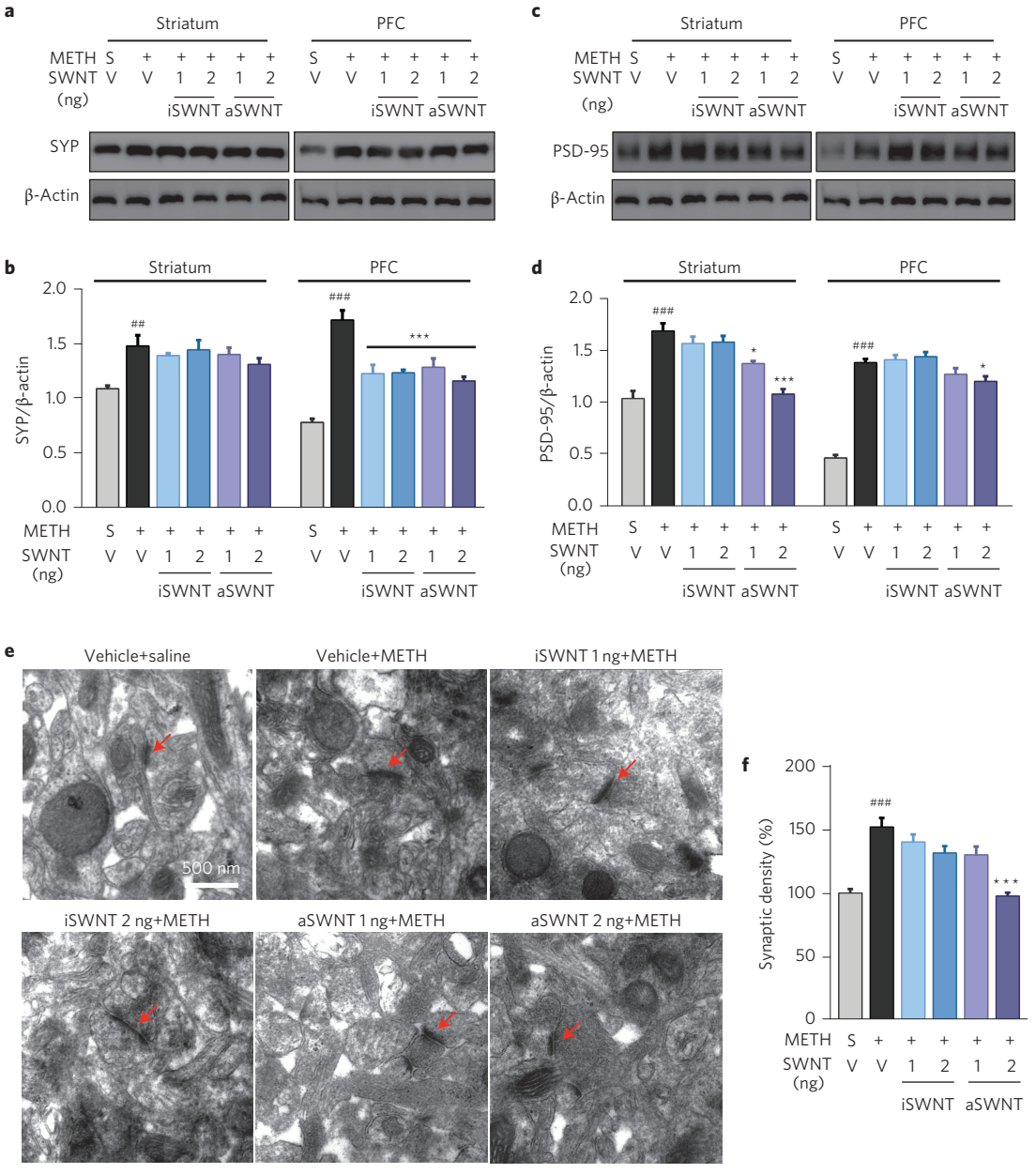

Figure 5 | Effects of METH and SWNTs on synaptic marker proteins and synaptic density in the striatum. a–d, Representative (**a**,**c**) and quantitative (**b**,**d**) Western immunoblot assays, illustrating that repeated METH treatment significantly increased the expression of SYP (**a**,**b**) and PSD-95 (**c**,**d**) in both the striatum and PFC ($n = 3$ mice per group). This increase was dose-dependently attenuated by SWNT pretreatment (**b**, striatum: $F_{5,12} = 22.53$, $p < 0.001$; PFC: $F_{5,12} = 4.66$, $p < 0.05$; **d**, striatum: $F_{5,12} = 28.05$, $p < 0.001$; PFC: $F_{5,12} = 21.20$, $p < 0.001$). **e**, Representative transmission electron microscope (TEM) images of synapses (marked by red arrows) in the striatum in the different treatment groups. **f**, Quantitative results of the synaptic density, illustrating that aSWNT pretreatment attenuated repeated METH-induced increases in synaptic density ($F_{5,114} = 16.57$, $p < 0.001$). The error bars indicate the s.e.m. of the mean values from 3 brain samples (from 3 animals) in each group. Each brain sample was replicated three times in Western blot assays (**b**,**d**). $^{\#\#}p < 0.01$, $^{\#\#\#}p < 0.001$, compared with the vehicle+saline group (grey bar). $^{*}p < 0.05$, $^{***}p < 0.001$, compared with the vehicle+METH group (black bar).

downwards (Fig. 3g). Similarly, aSWNTs also dose-dependently reduced [^{3}H]-dopamine re-uptake (Fig. 3h), suggesting that DAT may be another target acted on by SWNTs.

We next examined the effects of METH and SWNTs on the dopamine synthase (that is, on TH) and the dopamine degradation enzymes (such as monoamine oxidase (MAO) and catechol-O-methyltransferase (COMT)). We found that repeated METH administration (Fig. 4a) significantly upregulated TH expression in both the striatum and PFC (Fig. 4b). This is consistent with previous findings[15,16]. Pretreatment with SWNTs significantly reduced METH-enhanced TH expression in the striatum and PFC (Fig. 4c). In contrast to TH, neither METH nor SWNTs altered MAO or COMT activities in the striatum or PFC (Fig. 4d,e and Supplementary Fig. 5), suggesting a selective action on dopamine synthesis, but not on dopamine degradation.

Finally, we observed the effects of SWNTs on METH-induced synaptic plasticity as recent findings indicate that repeated exposure to METH produces neuroadaptative changes in the dendritic structure and synaptic connections in the striatum and PFC[17,18] that are thought to be associated with drug craving and relapse to drug-seeking behaviour[18]. We therefore examined the METH-induced changes in synaptic marker protein expression, including presynaptic synaptophysin (SYP) and postsynaptic density-95 (PSD-95). Figure 5 shows that repeated METH administration significantly

upregulated SYP (Fig. 5a,b) and PSD-95 (Fig. 5c,d) expression in both the striatum and PFC, which was attenuated by SWNT pre-treatment. Lastly, we used electron microscopy to observe the morphological changes in synapses where high densities of SYP and PSD-95 are expressed. A significant increase in the average synaptic density was observed in the brain after repeated METH treatments (Fig. 5e). This was also attenuated by aSWNTs in the striatum (Fig. 5e,f) and PFC (Supplementary Fig. 6).

In summary, the present study, for the first time, demonstrates that aSWNTs may have therapeutic potential for the treatment of METH dependence. This is based on the findings that aSWNTs not only inhibited the rewarding and psychomotor-stimulating effects of METH, but also inhibited METH- or cue-induced relapse to drug-seeking behaviour. These inhibitory effects seem to be dopamine-dependent as SWNTs significantly increased dopamine oxidation and attenuated METH-enhanced extracellular dopamine in the ventral striatum. In addition, SWNTs also inhibited [^{3}H]-WIN35,428 binding to DAT and [^{3}H]-dopamine reuptake, suggesting a possible interaction between SWNTs and DAT. However, another possible interpretation is that aSWNTs may also oxidize both of the radiolabelled compounds and therefore decrease the availability of radioligands in these assays. SWNTs also attenuated METH-enhanced expression of TH and the synaptic proteins SYP and PSD-95. The molecular mechanisms underlying these actions are unclear. A simple interpretation is that repeated METH administration causes massive dopamine release and depletes presynaptic dopamine, which leads to a series of adaptative changes in the synaptic structure or TH expression. Accordingly, the attenuation of METH-enhanced dopamine caused by SWNTs would counteract the METH-induced actions in protein expression. More studies are required to further address these issues.

A major concern about the use of SWNTs for the treatment of drug addiction is safety, particularly with regards to dopamine neuron toxicity after intracranial administration. At the doses used in the present study, we did not observe significant changes in general behaviours such as feeding, drinking, and locomotion. We also failed to observe significant neuronal toxicity in the striatum, PFC or midbrain after SWNT administration. Such low dopamine neurotoxicity may be related to the extremely low basal levels of extracellular dopamine ($<1 \times 10^{-9}$ M)[19,20], extremely low doses of SWNTs (1–2 ng) and high biocompatibility of SWNTs after intracranial administration[21,22].

As stated above, SWNTs have been widely used in recent biomedical research[23] due to their favourable properties, which include their large surface areas, superior bundle strength, highly electrical conductivity and, more importantly, their highly electrostatic attraction to dopamine[23,24]. We and others have recently started to explore the effects of SWNTs on the central nervous system[4,5,21], and most of these studies have focused on the neurotoxicity of SWNTs at high doses[25]. The present study provides the first proof-of-concept evidence that aSWNTs may be useful for the treatment of METH addiction. Therefore, these nanotubes deserve further research as a new approach for the treatment of drug abuse and addiction.

Methods

Methods and any associated references are available in the online version of the paper.

Received 3 November 2015; accepted 2 February 2016; published online 14 March 2016

References

1. Vocci, F. J. & Appel, N. M. Approaches to the development of medications for the treatment of methamphetamine dependence. *Addiction* **102,** 96–106 (2007).
2. Giraldo, J. P. *et al.* A ratiometric sensor using single chirality near-infrared fluorescent carbon nanotubes: application to in vivo monitoring. *Small* **11,** 3973–3984 (2015).
3. Khan, A. A. *et al.* Tunable scattering from liquid crystal devices using carbon nanotubes network electrodes. *Nanoscale* **7,** 330–336 (2015).
4. Xue, X. *et al.* Single-walled carbon nanotubes alleviate autophagic/lysosomal defects in primary glia from a mouse model of Alzheimer's disease. *Nano Lett.* **14,** 5110–5117 (2014).
5. Lee, H. J. *et al.* Amine-modified single-walled carbon nanotubes protect neurons from injury in a rat stroke model. *Nature Nanotech.* **6,** 121–125 (2011).
6. Ma, X. W. *et al.* Single-walled carbon nanotubes alter cytochrome *c* electron transfer and modulate mitochondrial function. *ACS Nano* **6,** 10486–10496 (2012).
7. Wang, L. R. *et al.* Structure-dependent mitochondrial dysfunction and hypoxia induced with single-walled carbon nanotubes. *Small* **10,** 2859–2869 (2014).
8. Figueiredo-Filho, L. C., Silva, T. A., Vicentini, F. C. & Fatibello-Filho, O. Simultaneous voltammetric determination of dopamine and epinephrine in human body fluid samples using a glassy carbon electrode modified with nickel oxide nanoparticles and carbon nanotubes within a dihexadecylphosphate film. *Analyst* **139,** 2842–2849 (2014).
9. Tiwari, J. N., Vij, V., Kemp, K. C. & Kim, K. S. Engineered carbon-nanomaterial-based electrochemical sensors for biomolecules. *ACS Nano* **10,** 46–80 (2016).
10. Yang, C., Denno, M. E., Pyakurel, P. & Venton, B. J. Recent trends in carbon nanomaterial-based electrochemical sensors for biomolecules: A review. *Anal. Chim. Acta.* **887,** 17–37 (2015).
11. Wise, R. A. Dopamine and reward: the anhedonia hypothesis 30 years on. *Neurotox. Res.* **14,** 169–183 (2008).
12. Chiu, V. M. & Schenk, J. O. Mechanism of action of methamphetamine within the catecholamine and serotonin areas of the central nervous system. *Curr. Drug Abuse Rev.* **5,** 227–242 (2012).
13. O'Brien, C. P. & Gardner, E. L. Critical assessment of how to study addiction and its treatment: Human and non-human animal models. *Pharmacol. Ther.* **108,** 18–58 (2005).
14. Pickens, C. L. *et al.* Neurobiology of the incubation of drug craving. *Trends Neurosci.* **34,** 411–420 (2011).
15. Keller, C. M. *et al.* Biphasic dopamine regulation in mesoaccumbens pathway in response to non-contingent binge and escalating methamphetamine regimens in the Wistar rat. *Psychopharmacology* **215,** 513–526 (2011).
16. Shepard, J. D., Chuang, D. T., Shaham, Y. & Morales, M. Effect of methamphetamine self-administration on tyrosine hydroxylase and dopamine transporter levels in mesolimbic and nigrostriatal dopamine pathways of the rat. *Psychopharmacology* **185,** 505–513 (2006).
17. Zhu, J. *et al.* Distinct roles of dopamine D3 receptors in modulating methamphetamine-induced behavioral sensitization and ultrastructural plasticity in the shell of the nucleus accumbens. *J. Neurosci. Res.* **90,** 895–904 (2012).
18. Robinson, T. E. & Kolb, B. Structural plasticity associated with exposure to drugs of abuse. *Neuropharmacology* **47,** 33–46 (2004).
19. Song, R. *et al.* Increased vulnerability to cocaine in mice lacking dopamine D3 receptors. *Proc. Natl Acad. Sci. USA* **109,** 17675–17680 (2012).
20. Xi, Z. X. *et al.* Brain cannabinoid CB_2 receptors modulate cocaine's actions in mice. *Nature Neurosci.* **14,** 1160–1166 (2011).
21. Arnold, M. S., Green, A. A., Hulvat, J. F., Stupp, S. I. & Hersam, M. C. Sorting carbon nanotubes by electronic structure using density differentiation. *Nature Nanotech.* **1,** 60–65 (2006).
22. Edwards, S. L., Werkmeister, J. A. & Ramshaw, J. A. M. Carbon nanotubes in scaffolds for tissue engineering. *Expert Rev. Med. Devices* **6,** 499–505 (2009).
23. Keefer, E. W., Botterman, B. R., Romero, M. I., Rossi, A. F. & Gross, G. W. Carbon nanotube coating improves neuronal recordings. *Nature Nanotech.* **3,** 434–439 (2008).
24. Suzuki, I., Fukuda, M., Shirakawa, K., Jiko, H. & Gotoh, M. Carbon nanotube multi-electrode array chips for noninvasive real-time measurement of dopamine, action potentials, and postsynaptic potentials. *Biosens. Bioelectron.* **49,** 270–275 (2013).
25. Bardi, G. *et al.* Functionalized carbon nanotubes in the brain: cellular internalization and neuroinflammatory responses. *PLoS ONE* **8,** e80964 (2013).

Acknowledgements

This work was supported by the National Key Scientific Project for New Drug Discovery and Development (2013ZX09301305), the National Natural Science Foundation key project (31430031), the National Distinguished Young Scholars grant (31225009) and the National Natural Science Foundation (No. 81373383) in China. This work was also supported by State High-Tech Development Plan (2012AA020804 and SS2014AA020708) and the National Institute on Drug Abuse (NIDA), Intramural Research Program (IRP), National Institutes of Health (NIH) in the United States of America. We also gratefully acknowledge support from the Chinese Academy of Sciences (CAS), Hundred Talents

Program (07165111ZX), the CAS Knowledge Innovation Program, the Strategic Priority Research Program of the Chinese Academy of Sciences (XDA09030301) and the external collaboration program of BIC, Chinese Academy of Science (121D11KYSB20130006). We thank I. Hanson for English editing services.

Author contributions

X.X., J.-Y.Y., Y.H., G.-L.G., Z.-X.X., C.-F.W. and X.-J.L. conceived and designed the experiments. X.X., Y.H., L.-R.W., P.L., L.-S.Y., G.-H.B., M.-M.Z., Y.-Y.L., X.-T.Y., X.-Y.F., X.-M.W. and W.C. performed the experiments. X.X., J.-Y.Y., Y.H., L.-R.W., R.-W.X., J.Q., H.-J.Z., Z.-X.X. and X.-J.L. analyzed the data. X.X. and L.-R.W. contributed materials/analysis tools. X.X., J.-Y.Y., Y.H., T.W., Z.-X.X. C.-F.W. and X.-J.L. wrote the paper. All authors discussed the results and commented on the manuscript.

Additional information

Supplementary information is available in the online version of the paper. Reprints and permissions information is available online at www.nature.com/reprints. Correspondence and requests for materials should be addressed to Z.X.X., C.F.W. and X.J.L.

Competing financial interests

The authors declare no competing financial interests.

Methods

Drugs. METH used in the self-administration and locomotion experiments was purchased from Sigma-Aldrich. METH (purity >98%) used in the CPP and neurochemical assays was obtained from the Liaoning Institute of Crime Detection and all other reagents were purchased from Sigma-Aldrich.

SWNT preparations. SWNTs were purchased from Chengdu Organic Chemicals, Chinese Academy of Sciences and further prepared as highly dispersed SWNTs, as described in our previous studies[7,26]. In brief, iSWNTs and aSWNTs were sorted by density gradient ultracentrifugation. A 0.2-ml-thick layer of highly dispersed SWNTs was put on top of a three-layer of water–iodixanol density gradient (10% + 30% + 60% iodixanol in water). Centrifugation was carried out in a P40ST swing bucket rotor in a Himac CP80WX ultracentrifuge (Hitachi High Technologies) at 20 °C with centripetal accelerations of about 200,000 *g* for 12 h. The bands containing separated SWNTs were manually retrieved from the centrifuge tube for subsequent characterization. All SWNT fractions were dissolved in 2 mg/ml sodium deoxycholate solution.

Atomic force microscopy. SWNTs were deposited by electrostatic adsorption onto mica. Freshly cleaved mica was pretreated with 2.0 mg ml^{-1} poly (diallyldimethylammonium chloride) (PDDA) for 1 h, and then soaked in the solution containing fractionated SWNTs for 30 min. This substrate was rinsed with water and then dried with air blowing. Atomic force microscopy measurements were performed on a Dimension 3,100 system (Digital Instruments) in tapping mode at room temperature (25–27 °C) and 20–30% humidity. About 50 SWNTs were measured to obtain the length distribution.

UV–visible–near-infrared absorption spectroscopy. Absorbance measurements in the UV–vis–near-infrared range were carried out using a LAMBDA 950 UV–VIS spectrophotometer (Perkin Elmer). Separated fractions were measured with further dilution in a 1 mm path quartz cuvette. A cuvette filled with water was used in a double-beam geometry to subtract the background due to water absorption.

Raman spectroscopy. Raman spectroscopy at 785 nm excitation was performed using a Renishaw micro-Raman spectroscopy system (Renishaw).

Animals. Male mice with C57BL/6J genetic backgrounds were used for the METH self-administration and locomotion experiments. Animals used for the CPP experiments were group-housed (3–5 per cage) in a fully accredited animal facility and were maintained on a reversed 12 h light/dark cycle with food and water available *ad libitum*. Male Swiss mice (initial body weight 22–24 g, 6–8 weeks old) were bred at the Experimental Animal Facility of Shenyang Pharmaceutical University and used for the CPP and other neurochemical assays. Intravenous METH self-administration experiments were performed at the National Institute of Drug Abuse (NIDA) in accordance with the National Research Council's Guide for the Care and Use of Laboratory Animals, and were approved by the NIDA Animal Care and Use Committee in the USA. All animal procedures conducted in China followed the Regulations of Experimental Animal Administration and were approved by the State Committee of Science and Technology of China.

Surgery and microinjection. The surgical procedures used for the (i.c.v.) guide cannula implantation and microinjection were the same as we reported previously[19,27]. The coordinates for the lateral ventricle are: anteroposterior –0.2 mm, mediolateral 1.0 mm, dorsoventral –2.5 mm^3. After 7 days of recovery from the surgery, the experiment began. SWNTs were initially suspended in 2 mg ml^{-1} sodium deoxycholate, and then diluted (0.5 mg ml^{-1}) to 1 or 2 μg ml^{-1} with artificial cerebrospinal fluid. A 1 μl aliquot of the SWNT solution was injected into the lateral ventricle over 2 min. The equivalent amount of sodium deoxycholate was used as the solvent vehicle.

Measurements of food intake, water intake and body weight. After habituation to the experimental conditions, daily food intake, water intake and body weight were measured beginning from one day before the guide cannula implantation surgery and lasting for 40 days. Mice were housed individually in the home cages and fed with a standard laboratory diet (HuaFukang) and tap water. The daily food or water intake was calculated by the total amounts that were given and the remaining amounts after 24 h of consumption.

Locomotor activity. Locomotor activity was measured in locomotor chambers (Model ZIL-2, Institute of Materia Medica, Chinese Academy of Medical Sciences, China) as previously reported[27]. Before the testing, mice were habituated to the apparatus for 60 min for 2 consecutive days without any drug injection. Locomotor activity was recorded for 1 or 2 h after SWNTs administration.

Intravenous METH self-administration. Animal surgery, drug self-administration apparatus, drug self-administration and i.c.v. microinjection procedures were the same as described previously[19,20]. In brief, after recovery from the surgery, each mouse was placed into a test chamber and allowed to lever-press for METH (0.05 mg kg^{-1} per infusion) delivered on a fixed-ratio 1 reinforcement schedule. Each METH infusion was associated with the presentation of a stimulus light and tone. During the infusion time, extra responses on the active lever were recorded but did not lead to extra infusions. After stable METH self-administration was achieved, the animals were randomly divided into three groups—vehicle ($n = 10$), 1 ng SWNTs ($n = 9$) and 2 ng SWNTs ($n = 9$) to examine the effects of SWNTs on METH self-administration (Fig. 1a). To avoid METH overdose, each animal was limited to a maximum of 50 METH injections per 3-hour-long testing session.

Cue-induced relapse to drug-seeking behaviour. After the completion of the above METH self-administration experiments, the animals were re-established for stable METH self-administration, followed by 3 weeks of withdrawal in the housing facility. On the test day, the mice were again placed into the self-administration chambers to observe METH-associated cue-induced lever-pressing (drug-seeking behaviour) in the presence or absence of SWNT pretreatment (0, 1 or 2 ng by i.c.v. microinjection given 30 min before the test). This cue-induced relapse test was repeated twice 2 days (T2) and 9 days (T3) after T1 in the absence of further aSWNT administration (Fig. 1a).

CPP. The experimental procedures for METH-induced CPP are the same as reported previously[28,29]. The pre-CPP test was performed to determine the amount of time that the animals spent in each chamber of the CPP device before METH administration. Animals that showed a significant preference (>10 min) for any particular environment in the pre-CPP test were excluded from the study. Each conditioning session includes METH-paired conditioning (1 h) and saline-paired conditioning (1 h) in a counterbalanced manner across all mice and chambers. During these sessions, mice were administered with METH (2 mg kg^{-1} by intraperitoneal (i.p.) injection every other day, and then were put into the METH-paired chambers for 1 h. Each animal received a total of 3 METH injections and 3 saline injections during the conditioning phase. Mouse CPP was recorded using a video camera and scored by a highly trained observer blinded to the treatments.

Effects of SWNTs on METH-induced CPP. After the pre-CPP test, one group of mice was randomly divided into 6 subgroups to observe the effects of the SWNTs on the acquisition of METH-induced CPP. In this study, SWNTs (0, 1 or 2 ng by i.c.v. microinjection) were given immediately before the first METH injection (Fig. 2a, Exp. 1).

Effects of SWNTs on CPP extinction. Another group of mice was used to observe the effects of SWNT pretreatment on the extinction response of METH-induced CPP (Fig. 2a, Exp. 2). In this experiment, each dose of SWNTs was given immediately before the first extinction session. During the extinction sessions animals were re-exposed to the same CPP chambers, but without METH or saline injections. The CPP scores were compared between the different treatment groups.

Effects of SWNTs on cue-induced CPP response. After METH-induced CPP was established, another group of mice underwent 10 days of withdrawal in their home cages in the animal facility. Then these animals were re-exposed to the same CPP chambers to observe the effects of SWNTs (0, 1 or 2 ng by i.c.v. microinjection 12 h before the test) on the METH-associated cue-induced CPP response (Fig. 2a, Exp. 3).

Effects of SWNTs on METH-induced reinstatement of CPP. After the acquisition and extinction of METH-induced CPP, another group of animals was used to observe the effects of SWNTs on the METH-induced reinstatement of CPP (Fig. 2a, Exp. 4). After METH (1 mg kg^{-1} by i.p. injection) was given, animals were placed in the same CPP chambers with access to either side for 15 min. METH-induced reinstatement of CPP were measured. At the end of the experiments, the mice were anesthetized and perfused with saline, and the brain was removed for the follow-up studies including Western blots, ELISA and histological synaptic density examination.

***In vivo* microdialysis.** The *in vivo* microdialysis procedures are the same as previously described[19,20,30]. In brief, *in vivo* microdialysis was performed in mice during the reinstatement test. The coordinates for the ventral striatum guide cannula implication are anteroposterior +1.4 mm, mediolateral ±2.0 mm, dorsoventral −3.5 mm. After 7 days of recovery from the surgery, a microdialysis probe was inserted into the ventral striatum via the pre-implanted guide cannula 12 h before microdialysis sample collection. SWNTs were given around 12 h before METH injection (that is, immediately before probing). After dialysate dopamine levels were stabilized, three baseline samples were collected, and then METH was given. Extracellular fluid samples were successively collected and simultaneously analysed every 20 min for 2–3 h after METH administration. After the completion of the experiments, mice were anesthetized and perfused transcardially with physiological saline followed by 10% paraformaldehyde. The locations of the tips of the dialysis probes were verified histologically. The procedures for the subsequent dialysate or tissue dopamine quantification were identical to those we have reported previously[19,20,30].

Standard hematoxylin and eosin (H&E) staining and TUNEL assay. H&E staining was used to determine possible neuronal death after SWNT administration. A

TUNEL staining kit (Roche Molecular Biochemicals) was used to detect DNA fragments (or cell death) according to the manufacturer's instruction.

Western immunoblot assays. At 2 h after the above METH-induced reinstatement of CPP test, mouse brains were perfused, and the striatum and PFC tissues were collected for Western blot assays ($n = 4$). The immunoblot procedures are the same as reported previously[19]. The following antibodies were used in this study: TH rabbit polyclonal antibody (Novus Biologicals, #NB300–109, 1:1,000), mouse anti-synaptophysin (SYP) monoclonal antibody (Chemincon, #MAB368, 1:1,000), anti-PSD-95 monoclonal antibody (Millipore, #4-1066, 1:1,000), DAT rabbit polyclonal antibody (Novus Biologicals, #NB300-254, 1:1,000), and β-actin (Cell signaling Technologies, #A2066, 1:1,000).

Immunohistochemistry. The procedures for TH- and DAT-immunostaining are the same as we reported previously[19]. Briefly, after brain perfusion and fixation, 20-μm-thick coronal sections were cut for immunohistochemistry assays. For immunofluorescent examination, the brain sections were first incubated with a 5% goat serum containing 0.2% Triton X-100 for 1 h, and then incubated with TH (1:500) and DAT (Millipore, #MAB369, 1:200) antibodies at 4 °C overnight. After being washed 3 times with PBS, the sections were incubated with Alexa-Fluor 488- and Alexa-Fluor 594-conjugated secondary antibodies (1:250, Invitrogen) for 1.5 h at room temperature, and then washed again with PBS. The TH- or DAT-immunostaining images were taken using a laser scanning confocal microscope (LSM 510 META, Carl Zeiss MicroImaging). The Image J software was then used for TH or DAT quantitative assays.

Synaptic density measurement. After brain perfusion at 24 h after the METH-induced reinstatement test, the striatum and PFC tissues were then dissected and fixed in 1% osmium tetroxide/1.25% potassium ferrocyanide in 0.15 M sodium phosphate buffer for 1 h. Samples were dehydrated in a graded ethanol series, followed by propylene oxide, and were infiltrated and embedded in Polybed 812 resin (Polysciences). Ultrathin (70 nm) sections were taken, mounted on 200 mesh copper grids and stained with uranyl acetate and lead citrate. The ultrathin sections were observed and photographed using a HT7700 transmission electron microscope (Hitachi High Technologies). Synapses were identified according to well-established criteria[31,32]. The synaptic density was measured quantitatively in both the striatum and PFC (~20 image fields from 4 mice in each group) according to methods described previously[32].

MAO activity assay. The PFC or striatum tissues were prepared using a mitochondrial extraction kit (Solarbio). After homogenization, brain tissue MAO activity was measured using a Monoamine Oxidase Assay Kit (Sigma). To determine the potential effects of SWNT on MAO activity, different doses of SWNTs were incubated with prepared tissues for 25 min. The specific MAO-B inhibitor pargyline was used as positive control. After the incubation, MAO reacted with p-tyramine, a substrate for MAO, resulting in the formation of H_2O_2, which was detected by a fluorimetric method (lex = 530/lem = 585 nm).

COMT activity assay. Brain tissue COMT activity was measured using an ELISA kit (Uscn Life Science). Briefly, protein samples were incubated with different doses of SWNTs for 20 min, and then COMT was reacted with a TMB substrate and a biotin-conjugated antibody specific to COMT. Horseradish peroxidase (HRP)-conjugated Avidin exhibited a change in colour, which was detected spectrophotometrically at a wavelength of 450 ± 10 nm.

[^{3}H]-dopamine uptake assay. Striatal tissues were homogenized with a Teflon glass homogenizer in ice-cold phosphate buffer and subsequently centrifuged at 1,000 *g* for 12 min at 4 °C. The resulting supernatant was centrifuged again at 12,500 *g* for 15 min to obtain the synaptosomal fraction. Synaptosomes were re-suspended at 50 mg ml^{-1} in an assay buffer (134 mM NaCl, 4.8 mM KCl, 1.3 mM $CaCl_2$, 1.4 mM $MgSO_4$, 3.3 mM NaH_2PO_4, 12.7 mM Na_2HPO_4, 11 mM glucose, and 1 mM ascorbic acid; pH 7.4) in the presence of 20 or 200 nM [^{3}H]-dopamine (specific activity: 40 Ci mmol^{-1}, Perkin Elmer Life Sciences). Eight concentrations of unlabelled dopamine were used to make a standard curve (data not shown). Ascorbic acid (10 μM) and pargyline (10 μM) were added to prevent monoamine and catecholamine oxidation and degradation. The striatal synaptosomes were incubated with or without SWNTs (0.05 ng mg^{-1} tissue) for 30 min at 37 °C. 5-HT (10 μM) reuptake inhibitor fluoxetine was added to the mixtures to prevent 5-HT transporter uptaking [^{3}H]-dopamine. Non-specific uptake was measured in the presence of 150 μM dopamine. Specific uptake was determined by subtraction of non-specific uptake from the total uptake. The reaction was stopped by adding 1 ml of ice-cold assay buffer, and the samples were rapidly filtered through Whatman GF/C glass microfibre filters (Brandel), washed three times with an ice-cold 0.32 M sucrose solution. The radioactivity on the filters was measured by micro-β 1450-Trilux using the liquid-scintillation counter mode. All samples were assayed in triplicate.

[^{3}H]-WIN35,428 binding assays. Striatal synaptosome preparation was the same as described above. The synaptosome pellets were then re-suspended at 100 mg ml^{-1} (wet weight of tissue) in the assay buffer and then incubated with different concentrations of [^{3}H]-WIN35,428 (~10 nM; Specific activity: 84 Ci mmol^{-1}, Perkin-Elmer Life Sciences, ranging between 0–10 nM) on ice for 60 min. The non-specific binding was obtained by using 30 μM benztropine. Ascorbic acid (10 μM) was added to block dopamine oxidation. Vacuum filtration with triple washes was performed using Whatman GF/C glass microfiber filters, and the resulting radioactivity on the filters was measured as described in the above [^{3}H]-dopamine uptake assay. All samples were assayed in triplicate and incubated at 4 °C for 120 min in the presence or absence of SWNTs (0.05 ng mg^{-1} striatal synaptosome tissue).

SWNT-coated electrode preparation. SWNTs were coated on indium tin oxide (ITO) electrodes using layer-by-layer adsorption. Cleaned ITO electrodes were first reacted with 10 μl of PDDA (2.0 mg ml^{-1} in a 10 mM phosphate buffer, pH 7.4) for 1 h and then washed carefully. The PDDA-coated electrode was then incubated with 10 μl of 0.05 mg ml^{-1} SWNTs in 10 mM phosphate (pH 7.4) for 1 h, and then washed carefully.

Electrochemical measurements. A CHI 660D workstation (CH Instruments) was used to collect electrochemical data. The measurements were performed using a three-electrode system. The SWNT-coated electrode served as the working electrode, a platinum wire was used as the auxiliary electrode, and the reference electrode was Ag/AgCl. All experiments were performed at room temperature in a phosphate buffer solution (10 mM, pH 7.4) as a background electrolyte.

Data analysis. All the data are expressed as mean ± s.e.m. The density of the immunoblot band was quantified using Image J software (NIH Image). The statistical significance was determined using one-way or two-way ANOVA. Dunnett's multiple comparison tests were used to analyse the between-group differences.

References

26. Wang, L., Zhang, L., Xue, X., Ge, G. L. & Liang, X. J. Enhanced dispersibility and cellular transmembrane capability of single-wall carbon nanotubes by polycyclic organic compounds as chaperon. *Nanoscale* **4,** 3983–3989 (2012).
27. Qi, J. *et al.* Inhibition by oxytocin of methamphetamine-induced hyperactivity related to dopamine turnover in the mesolimbic region in mice. *N. S. Arch. Pharmacol.* **376,** 441–448 (2008).
28. Qi, J. *et al.* Effects of oxytocin on methamphetamine-induced conditioned place preference and the possible role of glutamatergic neurotransmission in the medial prefrontal cortex of mice in reinstatement. *Neuropharmacology* **56,** 856–865 (2009).
29. Han, W. Y. *et al.* Oxytocin via its receptor affects restraint stress-induced methamphetamine CPP reinstatement in mice: involvement of the medial prefrontal cortex and dorsal hippocampus glutamatergic system. *Pharmacol. Biochem. Behav.* **119,** 80–87 (2013).
30. Qi, J. *et al.* A glutamatergic reward input from the dorsal raphe to ventral tegmental area dopamine neurons. *Nature Commun.* **5,** 5390 (2014).
31. Colonnier, M. & Beaulieu, C. An empirical assessment of stereological formulae applied to the counting of synaptic disks in the cerebral cortex. *J. Comp. Neurol.* **231,** 175–179 (1985).
32. DeFelipe, J., Marco, P., Busturia, I. & Merchan-Perez, A. Estimation of the number of synapses in the cerebral cortex: methodological considerations. *Cereb. Cortex.* **9,** 722–732 (1999).